



Increased Clinical Sensitivity and Specificity of Plasma Protein *N*-Glycan Profiling for Diagnosing Congenital Disorders of Glycosylation by Use of Flow Injection–Electrospray Ionization–Quadrupole Time-of-Flight Mass Spectrometry

Jie Chen,¹ Xueli Li,¹ Andrew Edmondson,² Gail Ditewig Meyers,¹ Kosuke Izumi,² Amanda M. Ackermann,³ Eva Morava,⁴ Can Ficicioglu,² Michael J. Bennett,^{1,5} and Miao He^{1,5*}

BACKGROUND: Congenital disorders of glycosylation (CDG) represent 1 of the largest groups of metabolic disorders with >130 subtypes identified to date. The majority of CDG subtypes are disorders of *N*-linked glycosylation, in which carbohydrate residues, namely, *N*-glycans, are posttranslationally linked to asparagine molecules in peptides. To improve the diagnostic capability for CDG, we developed and validated a plasma *N*-glycan assay using flow injection–electrospray ionization–quadrupole time-of-flight mass spectrometry.

METHODS: After PNGase F digestion of plasma glycoproteins, *N*-glycans were linked to a quinolone using a transient amine group at the reducing end, isolated by a hydrophilic interaction chromatography column, and then identified by accurate mass and quantified using a stable isotope-labeled glycopeptide as the internal standard.

RESULTS: This assay differed from other *N*-glycan profiling methods because it was free of any contamination from circulating free glycans and was semiquantitative. The low end of the detection range tested was at 63 nmol/L for disialo-biantennary *N*-glycan. The majority of *N*-glycans in normal plasma had <1% abundance. Abnormal *N*-glycan profiles from 19 patients with known diagnoses of 11 different CDG subtypes were generated, some of which had previously been reported to have normal *N*-linked protein glycosylation by carbohydrate-deficient transferrin analysis.

CONCLUSIONS: The clinical specificity and sensitivity of *N*-glycan analysis was much improved with this method. Additional CDGs can be diagnosed that would be missed by carbohydrate-deficient transferrin analysis. The assay provides novel biomarkers with diagnostic and potentially therapeutic significance.

© 2019 American Association for Clinical Chemistry

Congenital disorders of glycosylation (CDG)⁶ are genetic defects that affect processes in the synthesis of glycoconjugates. The majority of CDG subtypes are disorders of *N*-linked glycosylation, in which carbohydrate residues, known as *N*-glycans, are posttranslationally linked to the amino acid asparagine in peptides (Fig. 1) (1). The clinical presentation among patients with CDG is highly variable and difficult to diagnose (2). Although next-generation sequencing has advanced the diagnoses of CDG, functional or biochemical testing is still needed to confirm the diagnoses and for monitoring disease progression and management (2, 3).

The *N*-glycan profiles of secreted glycoproteins in plasma are highly heterogeneous. In addition to the complex glycans, there are also *N*-linked polymannose glycans, hybrids with both polymannose and sialylated antennae, and core fucosylated and/or bisecting glycans. Currently, carbohydrate-deficient transferrin (CDT) analysis is the primary biochemical test available for

¹ Division of Laboratory Medicine, The Children's Hospital of Philadelphia, Philadelphia, PA; ² Division of Human Genetics, Department of Pediatrics, The Children's Hospital of Philadelphia, Philadelphia, PA; ³ Division of Endocrinology and Diabetes, Department of Pediatrics, The Children's Hospital of Philadelphia, Philadelphia, PA; ⁴ Department of Clinical Genomics, Mayo Clinic, Rochester, MN; ⁵ Department of Pathology and Laboratory Medicine, University of Pennsylvania, Perelman School of Medicine, Philadelphia, PA.

* Address correspondence to this author at: Children's Hospital of Philadelphia, ARC 807c, 3401 Civic Center Blvd., Philadelphia, PA 19104. Fax 267-426-1295; e-mail hem@email.chop.edu.

This work was presented as an abstract at American Society for Mass Spectrometry 66th Annual Conference, San Diego, CA 2018.

Received September 13, 2018; accepted January 23, 2019.

Previously published online at DOI: 10.1373/clinchem.2018.296780

© 2019 American Association for Clinical Chemistry

⁶ Nonstandard abbreviations: CDG, congenital disorders of glycosylation; CDT, carbohydrate-deficient transferrin; QTOF, quadrupole time-of-flight; HILIC, hydrophilic interaction chromatography; IS, internal standard; PMM2, phosphomannomutase 2; ESI, electrospray ionization; ALG, asparagine-linked glycosylation; OST, oligosaccharyltransferase; SSR, signal sequence receptor; STT, subunit of the oligosaccharyltransferase complex; DDOST, dolichyl-diphosphooligosaccharide–protein glycosyltransferase; PGM1, phosphoglucomutase 1; CAD, carbamoyl-phosphate synthetase 2 aspartate transcarbamylase, and dihydroorotase; COP1, coat protein complex 1; COG, conserved oligomeric Golgi (complex); Gal-1-P, galactose-1-phosphate; Man0–9, GlcNAc2Man0–9.

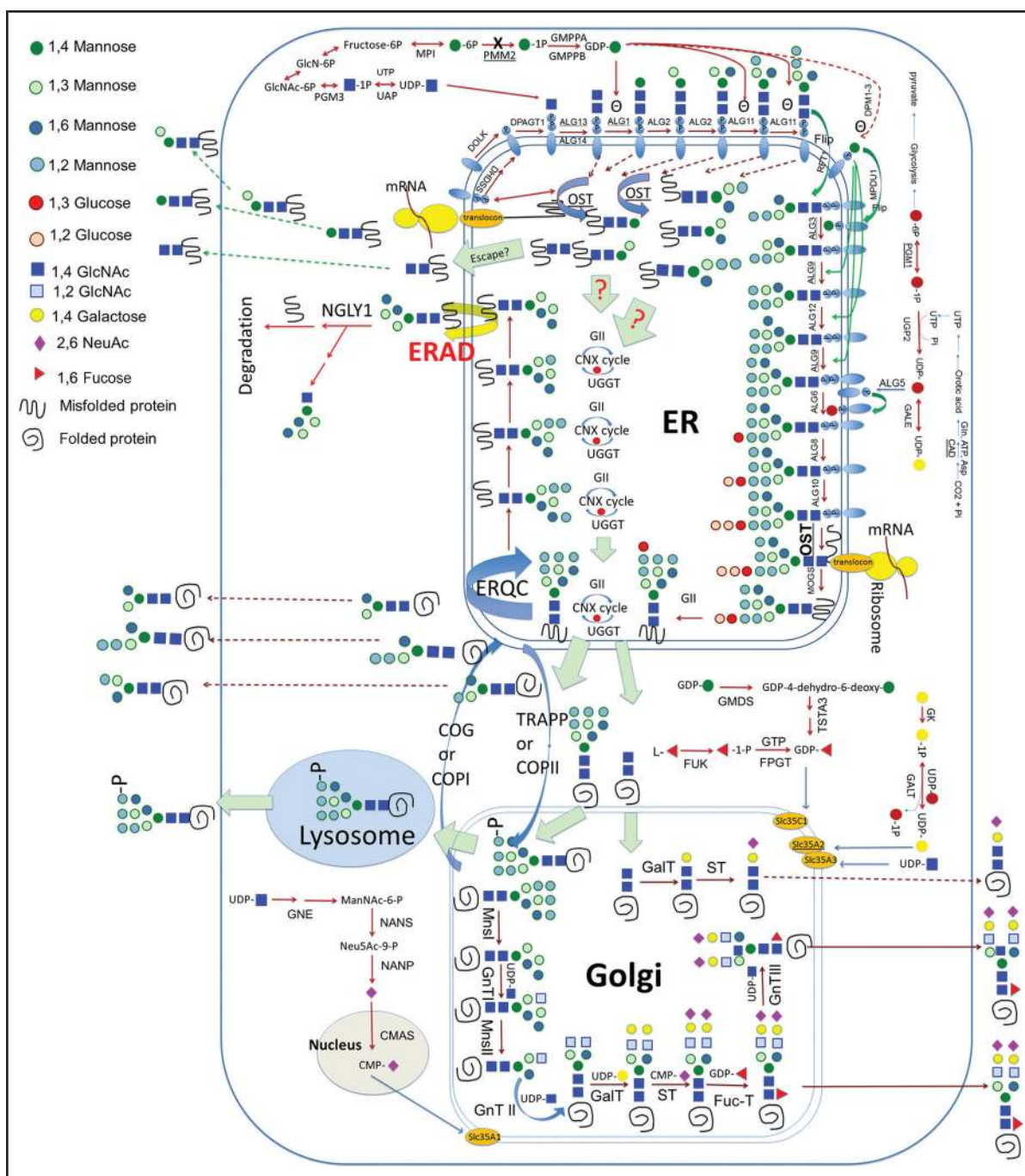


Fig. 1. A scheme of the N-linked glycosylation pathway.

ER, endoplasmic reticulum; ERAD, endoplasmic reticulum-associated degradation; ERQC, endoplasmic reticulum-associated protein quality control; GII, glucosidase II; CNX cycle, calnexin cycle; UGGT, UDP-glucose:glycoprotein glucosyltransferase; COG, conserved oligomeric Golgi complex; OST, oligosaccharyltransferase; COPI or II, coat protein complex I or 2; TRAPP, trafficking protein particle complex; MnsI or II, mannosidase I or II; GnT I, II, or III, GlcNAc transferase I, II, or III; GalT, galactosyltransferase; ST, sialyltransferase; FuT, fucosyltransferase; GlcN-6P, glucosamine-6-phosphate. Human genes shown in the figure: PMM2, MPI, GMPPA, GMPPB, PGM3, NGLY1, DOLK, DHDSS, DPAGT1, ALG13, ALG14, ALG1, ALG2, ALG11, RFT1, DPM1-3, MPDU1, ALG3, ALG9, ALG12, ALG6, ALG8, UGP2, GALE, ALG5, ALG10, MOGS, GMDS, TSTA3, GK, FPGT, FUK, SLC35C1, SLC35A2, SLC35A3, GNE, NANS, NANP, CMAS, PGM1, and CAD.

CDG diagnosis. Based on the changes of CDT, CDG can be grouped into 2 major types. Type I CDG refers to a reduction in the glycan occupancy of the glycosylation sites of transferrin; type II CDG refers to the loss of sialic acid residues of *N*-glycans on transferrin. However, transferrin has only complex glycans, which limits its application when testing for many CDG subtypes. Thus, multiple laboratories have described methods for the clinical application of plasma *N*-glycans to improve the diagnostic capability for CDGs (4, 5). We recently discovered novel *N*-linked di-, tri-, and tetra-saccharides that are diagnostic markers for the most common type I CDG subtypes (6). Although these small *N*-glycans are potentially biomarkers, they are prone to interferences from free glycans in the circulation and cannot be reliably measured quantitatively using existing *N*-glycan assays.

To overcome this limitation, we developed and validated a semiquantitative analysis of plasma *N*-glycans using a flow injection–electrospray ionization–quadrupole time-of-flight (QTOF) mass spectrometry method. An *N*-hydroxysuccinimide carbamate tag with a quinolone was added to the transient amine group at the reducing end of *N*-glycans after they were freshly released from glycoproteins using PNGase F enzyme. The labeled *N*-glycans were isolated by hydrophilic interaction chromatography (HILIC) and then identified by accurate mass (7). An isotope-labeled glycopeptide was added to each plasma sample as the internal standard (IS) to quantify or semiquantify targeted *N*-glycans. Because only *N*-glycans have the transient amine group, this method does not detect free circulating glycans, allowing accurate measurement of small peptide-linked *N*-glycans with low abundance. Because the analytical specificity and sensitivity of this assay improves identification, we expanded the *N*-glycan targets in normal plasma from 20 to 41, including many with abundance <1% of total glycan content, which could not be reliably identified or measured previously.

Here, we describe the characteristic *N*-glycan profiles of 17 patients with 10 different subtypes of CDG, as well as 2 patients with archain 1 (encoded by *ARCNI*⁷) deficiency and 1 patient with classic galactosemia.

Materials and Methods

MATERIALS AND INSTRUMENT

RapiFluor-MSTM *N*-Glycan Kit and HILIC 96-well μ ElutionTM plates were purchased from Waters. [¹³C]-sialylglycopeptide with >98% purity was purchased

from Omicron Biochemicals. Ammonium formate, acetonitrile, water, human [Glu¹]-fibrinopeptide B, and transferrin were purchased from Sigma Aldrich. Mass spectrometric analysis was performed on a Synapt G2 SiTM QTOF (Waters).

SAMPLES

Plasma samples from affected patients were either collected with consent as part of the integrated omics study of CDG protocol at the Children's Hospital of Philadelphia (Institutional Review Board 14–011223) or for routine clinical testing in the metabolic disease laboratory. Normal controls (n = 31) with an age range of 2 days to 65 years were either clinical samples with no known CDG diagnosis or collected from healthy adult volunteers. Of the control samples, 9 were from controls between the age of 2 days and 1 year old, 14 from controls between 1 and 18 years old, and 8 from controls >18 years old.

One patient with ALG3-CDG was diagnosed by abnormal transferrin and whole exome sequencing with homozygous R266C mutations. Six phosphomannomutase 2 (PMM2) patients were diagnosed by (a) characteristic *N*-glycan profiling with increased *N*-tetrasaccharide, Man₃, and Man₄GlcNAc₂; (b) deficient PMM2 enzymatic activity in leukocytes; and (c) targeted PMM2 gene sequencing showing each patient carrying 2 compound heterozygous mutations. One of the 6 PMM2 patients had whole exome sequencing. One ALG1 patient was previously described (8). She was diagnosed by abnormal *N*-glycan profile and mutations in *ALG1* gene. One ALG9 patient was diagnosed prospectively by *N*-glycan analysis, confirmed by targeted gene analysis and previously described (9). One patient with STT3B-CDG was diagnosed by whole exome sequencing. STT3B is the only disease-causing gene reported to carry 2 heterozygous predicted mutations, 1 inherited from the father and the other from the mother. DDOST and SSR4-CDG samples were positive control samples from Mayo Medical Laboratory with no molecular genetics data provided; the patient with PGM1-CDG was a published case diagnosed by enzymatic activity and mutations (10); the patient with CAD-CDG was the original patient published by Ng et al. (11); 3 SLC35A2 female patients were diagnosed by whole exome sequencing with de novo mutations; 2 *ARCNI* patients were published cases by Izumi (12). One classic GALT galactosemia patient was diagnosed by deficient red blood cell galactose-1-phosphate uridylyltransferase activity and homozygous *Q188R* mutations.

N-GLYCAN PREPARATION

N-Glycan preparation was carried out with a RapiFluor-MS *N*-Glycan Kit following the manufacturer's instructions. Briefly, 7.5 μ L of 10 \times diluted heparinized plasma,

⁷ Human genes: *ARCNI*, archain 1; *ALG1*, ALG1 chitobiosyl/diphosphodolichol beta-mannosyltransferase; *ALG3*, ALG3 alpha-1,3-mannosyltransferase; *ALG9*, ALG9 alpha-1,2-mannosyltransferase; *PMM2*, phosphomannomutase 2; *PGM1*, phosphoglucomutase 1; *SLC35A2*, solute carrier family 35 member A2.

7.5 μL of [^{13}C]-sialylglycopeptide (100 $\mu\text{g}/\text{mL}$), 6 μL of buffered RapiGest SFTM solution (5%, w/v), and 7.8 μL of water were mixed, heated at 90 °C for 3 min, and cooled to room temperature. Next, 1.2 μL of Rapid PNGase FTM was added to the mixture and incubated at 52 °C for 5 min and cooled to room temperature. Then 12 μL of RapiFluor-MS reagent in anhydrous dimethylformamide (6.9%, w/v) was added, incubated at room temperature for 5 min, and diluted with 358 μL of acetonitrile. A HILIC 96-well $\mu\text{Elution}$ plate operated on a vacuum manifold was used to isolate *N*-glycans. The wells were conditioned with 200 μL of water and then equilibrated with 200 μL of 85% acetonitrile/water (v/v). The sample was loaded into the wells and washed twice with 600 μL of 1% formic acid in 90% acetonitrile/water (v/v), before elution with 3×30 μL of elution buffer.

QTOF ANALYSIS

The mass spectrometric analysis was performed on the Waters' Synapt G2 Si QTOF in positive ion mode. Then, 2 μL of the *N*-glycan sample was delivered to the electrospray ionization (ESI) source through direct flow injection. Mobile phase A was 50 mmol/L ammonium formate, pH 4.4, and mobile phase B was 100% acetonitrile. Flow rate of 25% A and 75% B was set at 0.2 mL/min. Source temperature was 120 °C, and the desolvation temperature was 350 °C, with gas flow of 800 L/h. Cone and capillary voltage was 45 V and 3.0 kV, respectively. Data were acquired in resolution mode. Mass scan range was between 300 and 2000 *m/z*. Lockspray was used for mass calibration with 100 fmol/ μL [Glu¹]-fibrinopeptide B in 50% acetonitrile, 0.1% formic acid. The resolution used for this analysis was around 20000 full width at half maximum.

SEMIQUANTITATION AND CALCULATION

The IS was a custom-synthesized ^{13}C -labeled glycopeptide (product no. AAG-005) and commercially available at Omicron Biochemicals. This glycopeptide has a ^{13}C -labeled *N*-glycan, [$^{13}\text{C}_6$]-NeuAc₂Gal₃GlcNAc₄ with each NeuAc labeled with 3 ^{13}C , which is linked to the asparagine of the hexa-peptide NH₂-Lys-Val-Ala-Asn-Lys-Thr-COOH. Then, 750 ng of IS was added to each plasma sample. The intensities of each *N*-glycan species including the isotope-labeled *N*-glycan from the IS at *m/z* 1271.0199 were analyzed by NeoLynxTM. The concentration of the *N*-glycans was calculated as:

c = concentration

$$c_{N\text{-glycan}} = \frac{\text{Absolute Intensity}_{N\text{-glycan}}}{\text{Absolute Intensity}_{\text{internal standard}}} \times c_{\text{internal standard}}$$

Results

EXPANDED *N*-GLYCAN PANEL

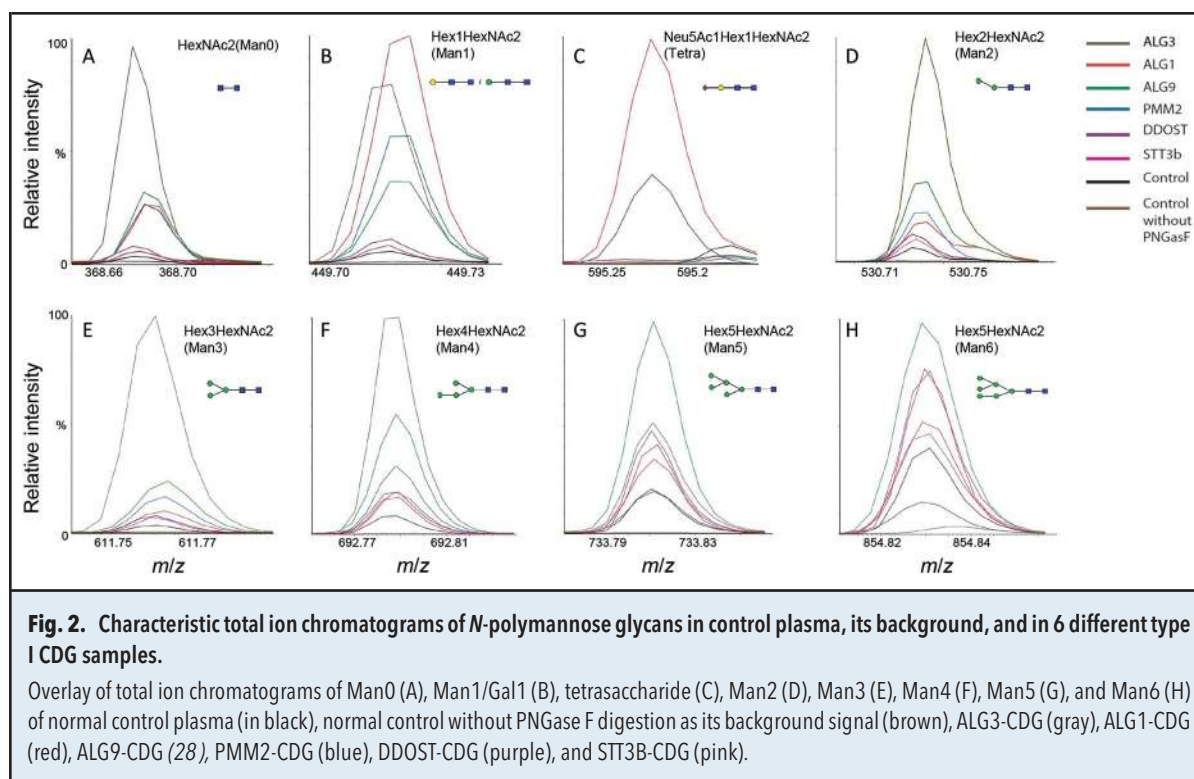
We used this assay to evaluate 53 unique *N*-glycans that have been identified in different human tissues in the consortium for functional glycomics database (13) or identified previously in CDG patients (4, 5). Both the observed and predicted mass of these glycans are shown in Table 1 of the Data Supplement that accompanies the online version of this article at <http://www.clinchem.org/content/vol65/issue5>. All the glycan ions evaluated had the fragment of the derivation tag and known glycan fragment ions as shown in Fig. 1 of the online Data Supplement. All the glycans were identified as protonated ions with 2 charges. Only the ions within 0.0001 *m/z* of the observed *m/z* were analyzed in plasma. The *m/z* difference between certain glycans such as Hex₁₂HexNAc₂ and Neu5Ac₂Fuc₁Hex₅HexNAc₄ was only 0.019. Thus, high mass accuracy was able to separate these species. Forty-one of these *N*-glycans, including 10 polymannose glycans, 14 complexed or hybrid glycans, and 17 core fucosylated and/or bisecting glycans, were consistently detected in normal human plasma, and more were detected in the plasma from known patients with CDG.

ANALYTICAL SPECIFICITY AND SENSITIVITY

To assess the analytical specificity of our assay for *N*-glycans, we measured the interference from free glycans by comparing the measurement of *N*-glycans with and without PNGase F digestion. As shown in Fig. 2, we did not detect any *N*-glycan signal in the control plasma samples without PNGase F digestion.

The linearity range of *N*-linked disialo-glycan at *m/z* 1298.0115 was measured using 0.005 to 20 g/L transferrin. The linearity range for this glycan was 2.6 to 506 $\mu\text{mol}/\text{L}$, which were released from 0.1 to 20 g/L transferrin (Table 1 and Fig. 3A). The low end of detection range tested for this *N*-glycan was 63 nmol/L. Another 27 *N*-glycan species from pure human transferrin were semi-quantified. Their linearity ranges are listed in Table 1 with the $R^2 > 0.99$ and the linearity curves of selected *N*-glycans shown in Fig. 3. The linearity curves of some minor glycans with similar abundance and structure had similar slopes and intercepts (Fig. 3, B and C), implying that these glycans had similar ionization properties and their quantity could be directly compared. The linearity curves of glycans with different structures had different slopes and intercepts, showing the presence of bias and potential interferences in the semiquantification process. More specific standards are required for their quantification (Fig. 3, D–F).

To better assess the linearity range for *N*-glycan species not detected on transferrin, a serial dilution (1–100 \times) of a plasma sample from a patient with ALG3-



CDG was performed. We found that the 45 *N*-glycans detected in this plasma all had a linear correlation of dilution with $R^2 > 0.99$ (see Table 2 in the online Data Supplement).

ASSAY IMPRECISION AND SAMPLE STABILITY

To study intraassay and interassay imprecision, we analyzed 3 different samples—purified human transferrin protein, normal plasma, and PMM2-CDG plasma—representing low, mid, and high abundance of diagnostic *N*-glycans, respectively (see Table 3 in the online Data Supplement). The intraassay ($n = 10$) CV of the majority of *N*-glycans was $<10\%$. The majority of the *N*-glycans also had an interassay CV ($n = 20$) of $<15\%$.

The stability of plasma or serum *N*-glycans was assessed by storing the whole blood or serum at room temperature for 0, 24, and 48 h. The *N*-glycan percentages in whole blood or serum were stable at room temperature for up to 48 h (see Table 4 in the online Data Supplement). The variability between plasma and serum was $<13\%$ CV with no particular trend.

REFERENCE RANGES

Reference ranges for plasma *N*-glycan abundance were collected with 31 controls with different ages and sex (see Table 5 in the online Data Supplement). Scatter plots of glycan abundance of these normal controls are shown in Fig. 4 in gray. The glycan abundance among normal

controls was distributed normally with no subgroups identified, consistent with previous experience (4).




















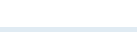




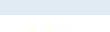



PMM2-CDG

PMM2-CDG is the most common subtype of CDG diagnosed worldwide. *PMM2* encodes phosphomannomutase 2 (PMM2). As many as 75% of patients diagnosed with CDG have mutations in *PMM2*; therefore, specific biomarkers are needed for expedited diagnosis and treatment monitoring of these patients (2).

Plasma samples from 6 PMM2-CDG patients were analyzed. Increased *N*-linked GlcNAc₂ Man_{2–4} (Man0–4) was detected in all of them with reduced Man7–9 abundance (Fig. 2 and Fig. 4A). The increase of Man3 and the ratio of Man4/6 were the consistent changes we detected among these patients (Fig. 4B; see also Table 5 in the online Data Supplement). In the 63-year old man with PMM2-CDG, the plasma values of Man3 were borderline high at 0.76% (reference, $<0.80\%$), as was the Man4/6 ratio at 0.59 (reference, <0.61), whereas the Man6/9 ratio was borderline low at 2.0 (reference, >2.1).

We previously reported that increased mannose-depleted Tetra (*N*-GlcNAc₂Gal₁Sial₁) are diagnostic and potentially therapeutic biomarkers for PMM2-CDG (6). The percentages of Tetra were increased in the plasma from 5 patients with PMM2-CDG (Figs. 2C and Fig. 4B; see also Table 5 in the online Data Supplement). Tetra was not detected in the plasma from one 63-year

Table 1. Linearity range of transferrin *N*-glycans.

Glycan	LR Tf ^a , mg/mL	LR glycan, μmol/L	R ²	Glycan	LR Tf, mg	LR glycan, μmol/L	R ²
	0.01-20	0.5-19.6	0.9975		1-10	0.3-1.6	0.9975
	0.01-20	1.5-69.3	0.9975		1.0-20	0.5-2.3	0.9991
	0.01-20	1.6-59.4	0.9982		1.0-20	0.06-0.40	0.9986
	0.01-20	2.6-12.1	0.9981		1.0-20	0.4-5.0	0.9969
	0.01-20	2.6-506.3 ^b	0.9922		1.0-20	0.02-0.44	0.9979
	0.01-10	0.8-9.8	0.9990		1.0-20	0.1-0.4	0.9905
	0.5-5	0.2-1.1	0.9930		1.0-10	0.09-0.40	0.9925
	0.1-20	0.7-5.1	0.9946		1.0-20	0.13-0.28	0.9922
	0.1-20	0.4-3.3	0.9982		1.0-20	0.03-0.8	0.9948
	0.1-10	0.4-1.4	0.9983		2.50-20	0.04-0.27	0.9913
	0.5-5	0.1-0.6	0.9954		2.50-20	0.04-0.20	0.9996
	0.5-20	0.1-1.1	0.9928		2.50-20	0.06-0.8	0.9948
	0.5-20	0.07-0.56	0.9986		2.50-20	0.03-0.26	0.9968
	0.5-20	0.2-0.7	0.9915		2.5-20	0.7-3.8	0.9998

^a LR, Linearity range; Tf, transferrin.
^b Linearity range of disialo-biantennary glycan is based on its concentration calculated from transferrin standard. All the other glycans' concentration on transferrin standard is unknown; thus, the semiquantified/measured concentration is shown.

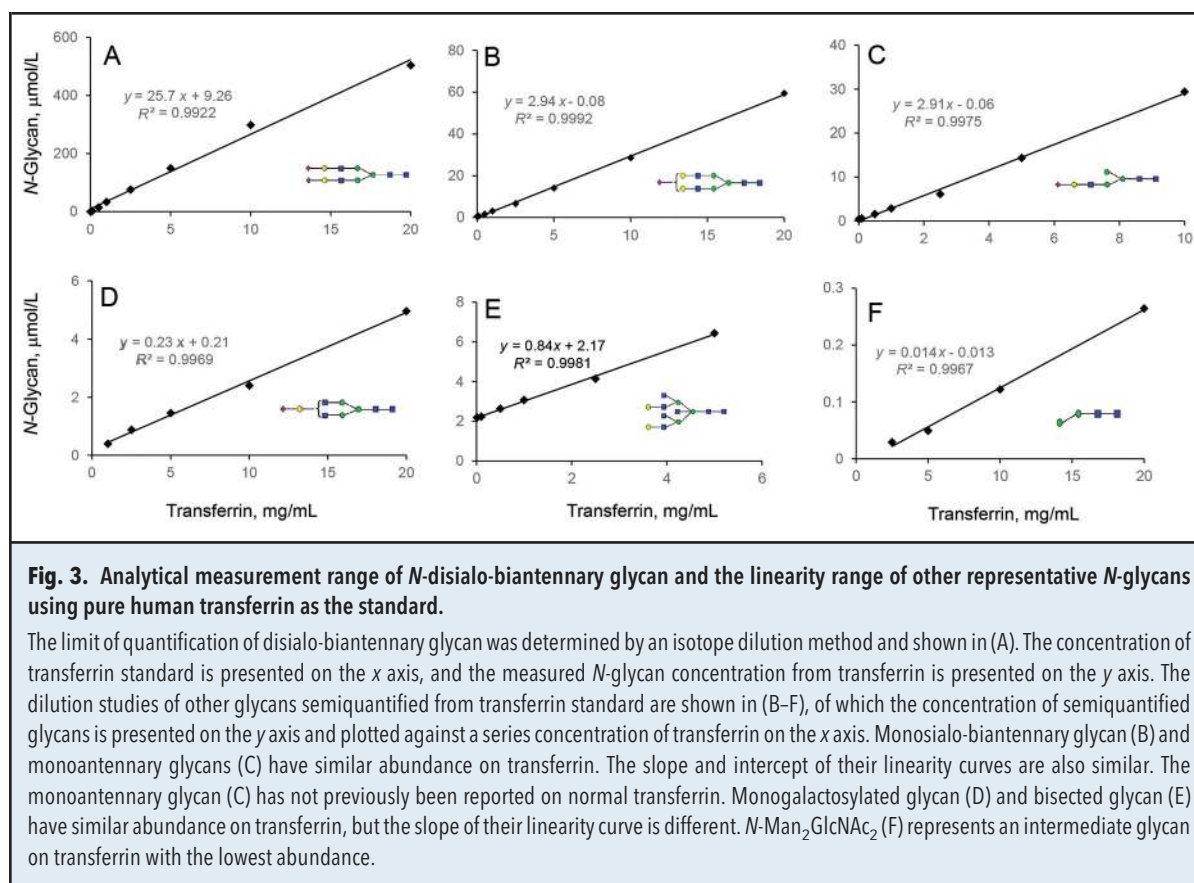
old patient with PMM2-CDG who had a very mild clinical phenotype. Comparing the total ion chromatogram of PMM2-CDG with those of other type I CDGs, the increases of Tetra, in combination with increased Man4/6 ratio differentiated PMM2-CDG from other type I CDGs (see Figs. 2, C, F, and H, and 4B). Interestingly, a previously unrecognized fucosylated monoantennary glycan at *m/z* 1012.89 was also increased in the majority of patients with PMM2-CDG (highlighted by the arrow in Fig. 4D).

OTHER TYPE I CDGS

Plasma *N*-glycan measurement of samples from 6 patients with 6 non-PMM2 type I CDGs were also obtained (Figs. 2 and 4; see also Table 5 in the online Data Supplement). In a patient with asparagine-linked glycosylation 1 (ALG1)-CDG, as anticipated based on our previous studies (6, 8), the abundance of mannose-

deficient Man0, Gal1, and Tetra was increased (Figs. 2, A–C, and 4, A and C; see also Table 5 in the online Data Supplement). The values for the other *N*-linked high mannose glycans were normal in ALG1-CDG. In multiple samples from 1 patient with ALG3-CDG, the abundance of *N*-linked Man0–4 is increased with reduced abundance of Man6 and Man8–9 (Figs. 2 and 4A; see also Table 5 in the online Data Supplement), consistent with the role of the enzyme encoded by *ALG3* in synthesizing Man6 from Man5 (Fig. 1). Tetra was absent in ALG3-CDG plasma (Fig. 2C).

In a sample from a single patient with ALG9-CDG, consistent with a previous report (9), *N*-linked Man0–6 (Fig. 2) were increased, with reduced abundance of Man8–9 (Fig. 4A; see Table 5 in the online Data Supplement). The observed very high ratio of Man6/9 and Man5/9 in plasma from this patient plasma is consistent



with the function of the enzyme encoded by *ALG9* in assembling Man8 and Man9 from Man6 in the endoplasmic reticulum (Fig. 1; see Table 5 in the online Data Supplement).

Translocon is the large protein complex that transports nascent polypeptides with a targeting signal sequence into the luminal space of the endoplasmic reticulum from the cytosol for glycosylation (Fig. 1). Deficiencies in components of translocon, including subunits of oligosaccharyl-transferase (OST) complex that transfer oligosaccharides from dolichol to the nascent protein and signal sequence receptors (SSR), can cause type I CDGs (14–16). Known CDG subtypes in this group are subunit 3 α of the oligosaccharyltransferase complex (STT3A)-CDG, STT3B-CDG, dolichyl-diphosphooligosaccharide–protein glycosyl-transferase (DDOST)-CDG, and SSR4-CDG (Fig. 1). These CDG subtypes are difficult to diagnose because the transferrin profiles are often normal. We measured plasma *N*-glycan profiles of 1 patient with STT3B-CDG, 1 patient with DDOST-CDG, and 1 patient with SSR4-CDG. We detected increases of Man4–8 abundance in the STT3B-CDG plasma (Fig. 2; see also Table 5 in the online Data Supplement). Similarly, increased abundance of Man4–6 and Man9 was detected in the

DDOST-CDG plasma (Figs. 2 and Fig. 4A; see also Table 5 in the online Data Supplement). Mildly increased Man5 and Man6 abundance and Man9/2 ratio were also detected in the plasma sample from a patient with SSR4-CDG, although such increases in SSR4-CDG were lower than those in STT3B-CDG or DDOST-CDG (Fig. 2; see Table 5 in the online Data Supplement). Thus, the common abnormal *N*-polymannose could potentially be used to confirm deficiencies in translocon.

TYPE II CDG

The plasma *N*-glycan profile has been reported to be optimal for detecting glycosylation changes in patients with type II CDG (3, 4). To test the clinical sensitivity of our new method, we generated plasma *N*-glycan profiles from samples from 5 patients with CDG type II. Four of these 5 samples had previously been shown to have normal CDT profiles.

Phosphoglucomutase 1 (PGM1)-CDG shows mixed type I and type II CDG pattern by CDT analysis. Oral galactose supplementation improves protein glycosylation in these patients, and their CDT profiles often fluctuate close to or within normal ranges posttreatment

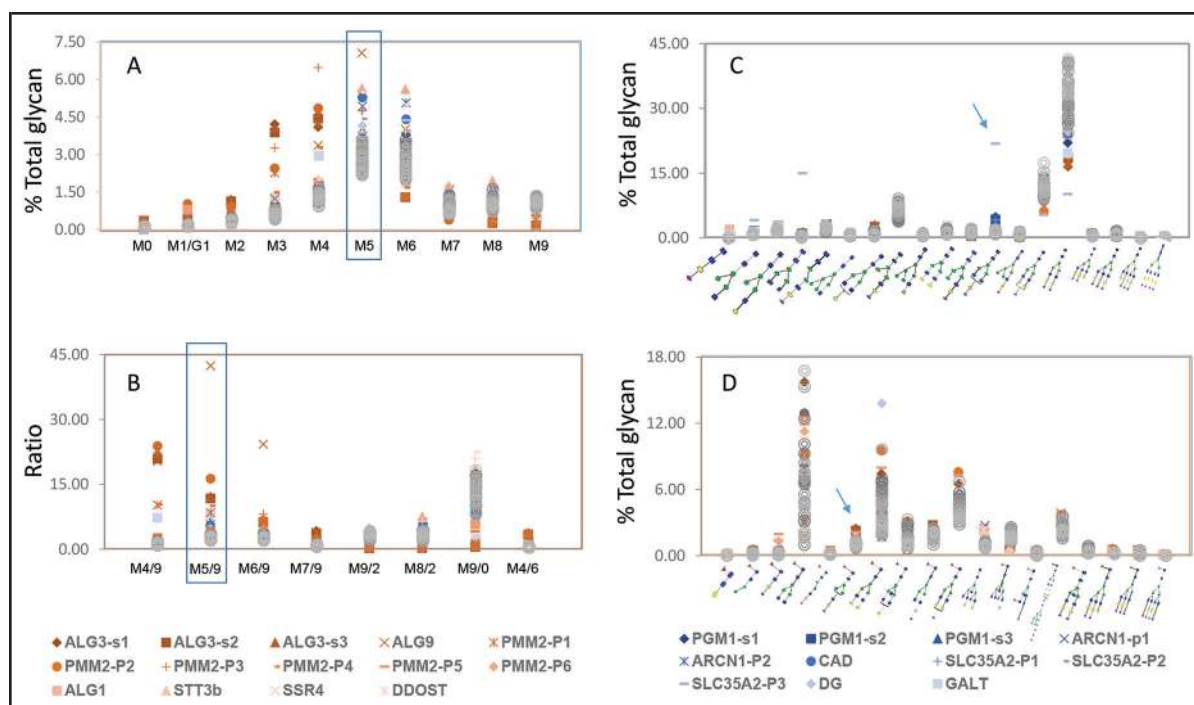


Fig. 4. Plasma *N*-glycan levels in type I and type II CDG patients compared with normal controls.

(A), The overlays of plasma *N*-high mannose abundance (% total glycan) in type I CDG patients (red), type II CDG patients (blue), and 31 normal controls (gray). (B), Selected ratios between *N*-linked high mannose among type I CDG patients, type II CDG, and normal controls. (C), Plasma *N*-linked complexed glycan levels in type I CDG patients, type II CDG, and normal controls. (D), Plasma *N*-linked fucosylated and bisected *N*-glycan levels in type I CDG patients, type II CDG, and normal controls. The abundance of *N*-linked Man5 (A) and the ratio of Man5/Man9 (B), highlighted by blue rectangles, separate most CDG patients from the normal controls. Among complexed glycans, the abundance of 2 monogalactosylated glycans (highlighted by blue arrows) separates most patients with CDG from the normal controls (C). A fucosylated monoantennary glycan and a monogalactosylated glycan (highlighted by blue arrows) are representative plasma *N*-glycan markers that separate patients with CDG from normal controls.

(10, 17). The plasma *N*-glycan profiles from a patient with PGM1-CDG, who was on a trial of galactose therapy as described before (10), were analyzed. *N*-Glycan abundance in samples collected after >3 months of 0.5, 1, and 1.5 g/kg/day D-galactose supplement are shown in Table 2. Although the CDT profiles fluctuated within normal limits, all the samples showed abnormal *N*-glycan

abundance with increased abundance of monogalactosylated glycans at *m/z* 1049.91. We observed minimum fluctuation in *N*-glycan abundance between samples that were collected at different time points with the same therapy. The agalactosylated and monogalactosylated glycan abundance, Man9/0, and monogalactosylated/disialo glycan ratios trended toward normal in a dose-dependent

Table 2. *N*-Glycan changes in a PGM1-CDG patient on different doses of galactose therapies.

<i>N</i> -Glycan abundance	Agalactosylated glycan	Monogalactosylated glycan	Man9/Man0	Mono-gal/di-sialo biantennary
Control	0.08%–0.61%	0.82%–1.98%	8.2%–18.2%	0.02–0.07
PGM1-CDG (0.5 g/kg galactose)	0.75 ± 0.17 ^a	4.41 ± 0.14	8.79	0.21
PGM1-CDG (1.0 g/kg galactose)	0.48 ± 0.11	3.53 ± 0.31	9.06	0.16
PGM1-CDG (1.5 g/kg galactose)	0.44 ± 0.08	3.46 ± 0.14	15.91	0.12

^a Mean of *N*-glycan measurement of at least 3 plasma samples collected on different days.

manner with the increase of galactose supplementation. These findings support that our semiquantitative *N*-glycan analysis could be used to monitor PGM1-CDG patient response to galactose therapy more optimally than the use of CDT monitoring.

Solute Carrier Family 35 Member A2 (SLC35A2)-CDG results from an X chromosome-linked deficiency in a Golgi UDP-galactose transporter. Most patients with SLC35A2-CDG are females with early infantile epileptic encephalopathy, many of whom carry de novo heterozygous mutations. CDT profiles are reportedly normal in many of them (18, 19). Interestingly, in 1 female SLC35A2-CDG patient who was reported to have abnormal CDT, CDT improved rapidly with oral galactose supplementation (20). Thus, a more clinical sensitive and consistent biomarker for this disease is needed. The *N*-glycan profiles of multiple plasma samples from 3 known female patients with SLC35A2-CDG were obtained, and all samples showed persistent increases in monogalactosylated or agalactosylated glycans. In addition, mildly increased *N*-Man5 and Man5/9 were also noted, with reduced or borderline low Man9 abundance (Fig. 4) (21). CDT profiles of 2 of the 3 patients were normal.

Carbamoyl-phosphate synthetase 2 aspartate transcarbamylase and dihydroorotase (CAD)-CDG is a deficiency in cytosolic trifunctional enzyme that contains carbamoyl-phosphate synthetase 2, aspartate transcarbamylase, and dihydroorotase activities. The affected patient has a persistently low urine orotic acid concentration, ranging from 0.11 to 0.19 mmol/mol creatinine (reference, 1.12–2.52), and reduced UDP-galactose and UDP-GlcNAc production (11). The CDT profile has been reported to be normal in CAD-CDG. We identified mild hypogalactosylation of plasma *N*-glycans in the patient before uridine supplementation (not shown). After uridine treatment, which is the therapeutic option for this disorder, we still saw a borderline increase of monogalactosylated glycan at 2.88% (reference, <1.98), along with reduced disialo-biantennary glycan at 23.9% (reference, >24.3). Thus, the *N*-glycan changes in CAD-CDG support persistent hypogalactosylation as a biochemical feature of this disease (Fig. 4C).

Heterozygous loss of function mutations in *ARCNI* cause a disorder characterized by facial dysmorphism, severe micrognathia, microcephaly, rhizomelic short stature, and developmental delay (12). *ARCNI* encodes the subunit δ of coat protein complex 1 (COP1). Similar to the conserved oligomeric Golgi (COG) complex, COP1 coats vesicles that retrograde transport proteins from Golgi to endoplasmic reticulum and influences the Golgi structural integrity and processing activity. Because most genetic defects in COG complex subunits are type II CDGs, we hypothesized that a defect in COP1 coatomer would also affect protein glycosylation. We tested plasma

samples from 2 patients with *ARCNI* mutations. Both showed borderline increases of Man5 accompanied by mild reductions in Man9, leading to increased Man5/9 ratios. These changes are similar to the known polymannose changes in patients with COG4 or COG7-CDG (4).

SECONDARY GLYCOSYLATION CHANGES IN CLASSIC GALACTOSEMIA PATIENTS

Classic galactosemia is caused by mutations in the galactose-1-phosphate uridylyltransferase gene that encodes an enzyme that facilitates the conversion of UDP-glucose and galactose-1-phosphate (Gal-1-P) to UDP-galactose and glucose-1-phosphate. Secondary glycosylation changes have been reported in patients with uncontrolled classic galactosemia (22). We tested a plasma sample from a 5-day-old patient with homozygous Q188R mutations in the galactose-1-phosphate uridylyltransferase gene before the initiation of the treatment. The red blood cell Gal-1-P concentration was 138 mg/dL hemoglobin (reference, <1.5 mg/dL). Quantitative *N*-glycan analysis of the same sample showed increased Man0–4 and decreased Man6, Man8, and Man9 (see Table 5 in the online Data Supplement). The abundance of Man9 was reduced at 0.39% (reference, 0.82–1.36) whereas the Man5/9 ratio was increased at 8.04 (reference, 2.07–3.54). The disialo-biantennary glycan was also reduced at 19.5% (reference, 24.3–41.4). In addition, the mannose-deprived Tetra was also increased at 0.36% (reference, 0), indicating a functional deficiency in GDP-mannose. Unexpectedly, the hypogalactosylated glycans were not increased in this patient with classic galactosemia and monogalactosylated biantennary glycan at 0.94% (reference, 0.82–1.98). Thus, untreated galactosemia patients may have *N*-glycan profiles that are very similar to *PMM2*-CDG.

Discussion

We developed a new semiquantitative *N*-glycan assay (ESI-QTOF) to improve the diagnostic capacity of CDG. We found that *N*-polymannose abundance is a clinical sensitive biomarker for screening most CDG subtypes that we tested and more clinical sensitive biomarkers than CDT in certain subtypes. Glycoproteins with *N*-linked polymannose glycans are not subject to the clearance by asialoglycoprotein receptors in liver and, thus, have a more stable presence in the circulation than transferrin. We demonstrated previously described diagnostic *N*-glycan changes in ALG1-, *PMM2*-, and ALG9-CDG with our new ESI-QTOF assay. We also described novel potentially characteristic polymannose changes in ALG3-, STT3B-, DDOST-, and SSR4-CDGs. Most of the patients with CDG that we tested have a high Man5/9 ratio, supporting the Man5/9 ratio as an

informative biomarker for screening most of the common CDG subtypes.

Man0 was initially described in cancerous cells during glucose deprivation (23). We first reported the presence of Man0 in ALG1-CDG patients (6). In this study, we found that there was marked increases of Man0 in patients with ALG3-CDG and ALG9-CDG without any trace of Tetra, showing that proteins with the modification of Man0 in these CDG subtypes are secreted into the circulation without entering the glycan processing pathway in the Golgi. In renal carcinoma cells, Man0-modified proteins are known to induce G2/M arrest and cell death with prolonged upregulation of the unfolded protein response (24). Whether the Man0-modified secreted proteins in the plasma of these patients with CDG are toxic unfolded proteins is important to investigate in the future.

Although asialoglycoproteins are subject to clearance from the circulation by asialoglycoprotein receptors, mild increases of asialoglycans were readily detected in all the known patients with type II CDGs using the *N*-glycan analysis by ESI-QTOF, despite persistently normal profile of CDT. Thus, the clinical sensitivity of our test for detecting changes in the same type of complex glycans in patients is also much higher than that of CDT analysis. In a patient with *PGM1*-CDG, our analysis of *N*-glycans was able to detect changes that correlated with therapies, suggesting that there is a therapeutic potential in these biomarkers.

Because there are >900 genes in humans that encode for proteins directly involved in glycosylation processes, many factors that alter the expression of these genes are not yet known. With the increased clinical sensitivity of our *N*-glycan assay, we also expect to see an increase in secondary findings, some of which could be related to the altered proportion of major glycoproteins in the circulation or epigenetic regulation in inflammatory conditions, liver dysfunction, or cancer (25–27), and some could be secondary to a genetic condition that alters gene expression, cellular protein trafficking, or membrane dynamics of the Golgi or endoplasmic retic-

ulum, all processes that could affect protein glycosylation (2).

Author Contributions: All authors confirmed they have contributed to the intellectual content of this paper and have met the following 4 requirements: (a) significant contributions to the conception and design, acquisition of data, or analysis and interpretation of data; (b) drafting or revising the article for intellectual content; (c) final approval of the published article; and (d) agreement to be accountable for all aspects of the article thus ensuring that questions related to the accuracy or integrity of any part of the article are appropriately investigated and resolved.

A. Edmondson, provision of study material or patients; G. Ditewig Meyers, statistical analysis; A.M. Ackermann, provision of study material or patients; E. Morava, provision of study material or patients; C. Ficicioglu, provision of study material or patients; M. He, statistical analysis, administrative support, provision of study material or patients.

Authors' Disclosures or Potential Conflicts of Interest: Upon manuscript submission, all authors completed the author disclosure form. Disclosures and/or potential conflicts of interest:

Employment or Leadership: A. Edmondson, Children's Hospital of Philadelphia; M.J. Bennett, *Clinical Chemistry*, AACC.

Consultant or Advisory Role: None declared.

Stock Ownership: None declared.

Honoraria: None declared.

Research Funding: Ellie's CDG research fund.

Expert Testimony: None declared.

Patents: None declared.

Role of Sponsor: The funding organizations played no role in the design of study, choice of enrolled patients, review and interpretation of data, preparation of manuscript, or final approval of manuscript.

Acknowledgments: The authors thank Dr. Kimiyo Raymond (Mayo Clinic, Rochester, MN) for providing plasma samples from patients with known diagnosis of DDOST-CDG and SSR4-CDG. The authors also thank Amul C. Shah for coordinating study material. The authors thank all the current clinical technologists in the Michael J. Palmieri Metabolic Disease Laboratory for their contributions. The authors also thank Richard Earley from Waters Corporation and Qingfeng Pan from Omicron Biochemicals who provided technical consult relevant to this study. The study is partially funded by Ellie's CDG research fund, a gift to the Children's Hospital of Philadelphia. The authors thank all the CDG patients and their families for their support of this research.

References

1. Ng BG, Freeze HH. Perspectives on glycosylation and its congenital disorders. *Trends Genet* 2018;34:466–76.
2. Peanne R, de Lonlay P, Foulquier F, Kornak U, Lefeber DJ, Morava E, et al. Congenital disorders of glycosylation (CDG): quo vadis? *Eur J Med Genet* 2018;61:643–63.
3. Van Scherpenzeel M, Willems E, Lefeber DJ. Clinical diagnostics and therapy monitoring in the congenital disorders of glycosylation. *Glycoconj J* 2016;33:345–58.
4. Xia B, Zhang W, Li X, Jiang R, Harper T, Liu R, et al. Serum *N*-glycan and *O*-glycan analysis by mass spectrometry for diagnosis of congenital disorders of glycosylation. *Anal Biochem* 2013;442:178–85.
5. Saldova R, Stockmann H, O'Flaherty R, Lefeber DJ, Jaeken J, Rudd PM. *N*-Glycosylation of serum IgG and total glycoproteins in MAN1B1 deficiency. *J Proteome Res* 2015;14:4402–12.
6. Zhang W, James PM, Ng BG, Li X, Xia B, Rom J, et al. A novel *N*-tetrasaccharide in patients with congenital disorders of glycosylation, including asparagine-linked glycosylation protein 1, phosphomannomutase 2, and mannose phosphate isomerase deficiencies. *Clin Chem* 2016;62:208–17.
7. Lauber MA, Yu YQ, Brousmiche DW, Hua Z, Koza SM, Magnelli P, et al. Rapid preparation of released *N*-glycans for HILIC analysis using a labeling reagent that facilitates sensitive fluorescence and ESI-MS detection. *Anal Chem* 2015;87:5401–9.
8. Ng BG, Shiryayev SA, Rymen D, Eklund EA, Raymond K, Kircher M, et al. ALG1-CDG: clinical and molecular characterization of 39 unreported patients. *Hum Mutat* 2016;37:653–60.
9. Davis K, Webster D, Smith C, Jackson S, Sinasac D, Seargeant L, et al. ALG9-CDG: new clinical case and review of the literature. *Mol Genet Metab Rep* 2017;13:55–63.
10. Wong SY, Gadomski T, van Scherpenzeel M, Honzik T, Hansikova H, Holmefjord KSB, et al. Oral D-galactose supplementation in PGM1-CDG. *Genet Med* 2017;19:1226–35.
11. Ng BG, Wolfe LA, Ichikawa M, Markello T, He M, Tiffit CJ, et al. Biallelic mutations in CAD, impair de novo pyrim-

- idine biosynthesis, and decrease glycosylation precursors. *Hum Mol Genet* 2015;24:3050–7.
12. Izumi K, Brett M, Nishi E, Drunat S, Tan ES, Fujiki K, et al. ARCN1 mutations cause a recognizable craniofacial syndrome due to COPI-mediated transport defects. *Am J Hum Genet* 2016;99:451–9.
 13. Consortium for functional glycomics. CFG data. <http://www.functionalglycomics.org/glycomics/publicdata/home.jsp> (Accessed January 2017).
 14. Jaeken J, Peanne R. What is new in CDG? *J Inherit Metab Dis* 2017;40:569–86.
 15. Jones MA, Ng BG, Bhide S, Chin E, Rhodenizer D, He P, et al. DDOST mutations identified by whole-exome sequencing are implicated in congenital disorders of glycosylation. *Am J Hum Genet* 2012;90:363–8.
 16. Shrimal S, Ng BG, Losfeld ME, Gilmore R, Freeze HH. Mutations in STT3A and STT3B cause two congenital disorders of glycosylation. *Hum Mol Genet* 2013;22:4638–45.
 17. Nolting K, Park JH, Tegtmeier LC, Zuhlsdorf A, Gruneberg M, Rust S, et al. Limitations of galactose therapy in phosphoglucomutase 1 deficiency. *Mol Genet Metab Rep* 2017;13:33–40.
 18. Ng BG, Buckingham KJ, Raymond K, Kircher M, Turner EH, He M, et al. Mosaicism of the UDP-galactose transporter SLC35A2 causes a congenital disorder of glycosylation. *Am J Hum Genet* 2013;92:632–6.
 19. Kodera H, Nakamura K, Osaka H, Maegaki Y, Haginoya K, Mizumoto S, et al. De novo mutations in SLC35A2 encoding a UDP-galactose transporter cause early-onset epileptic encephalopathy. *Hum Mutat* 2013;34:1708–14.
 20. Dorre K, Olczak M, Wada Y, Sosicka P, Gruneberg M, Reunert J, et al. A new case of UDP-galactose transporter deficiency (SLC35A2-CDG): molecular basis, clinical phenotype, and therapeutic approach. *J Inherit Metab Dis* 2015;38:931–40.
 21. Maszszak-Seneczko D, Sosicka P, Kaczmarek B, Majkowski M, Luzarowski M, Olczak T, et al. UDP-galactose (SLC35A2) and UDP-N-acetylglucosamine (SLC35A3) transporters form glycosylation-related complexes with mannoside acetylglucosaminyltransferases (Mgats). *J Biol Chem* 2015;290:15475–86.
 22. Liu Y, Xia B, Gleason TJ, Castaneda U, He M, Berry GT, et al. N- and O-linked glycosylation of total plasma glycoproteins in galactosemia. *Mol Genet Metab* 2012;106:442–54.
 23. Isono T. O-GlcNAc-specific antibody CTD110.6 cross-reacts with N-GlcNAc2-modified proteins induced under glucose deprivation. *PLoS One* 2011;6:e18959.
 24. Isono T, Chano T, Kitamura A, Yuasa T. Glucose deprivation induces G2/M transition-arrest and cell death in N-GlcNAc2-modified protein-producing renal carcinoma cells. *PLoS One* 2014;9:e96168.
 25. de Jong SE, Selman MH, Adegnikaa AA, Amoah AS, van Riet E, Kruize YC, et al. IgG1 Fc N-glycan galactosylation as a biomarker for immune activation. *Sci Rep* 2016;6:28207.
 26. Clarke JD, Novak P, Lake AD, Hardwick RN, Cherrington NJ. Impaired N-linked glycosylation of uptake and efflux transporters in human non-alcoholic fatty liver disease. *Liver Int* 2017;37:1074–81.
 27. Lan Y, Hao C, Zeng X, He Y, Zeng P, Guo Z, et al. Serum glycoprotein-derived N- and O-linked glycans as cancer biomarkers. *Am J Cancer Res* 2016;6:2390–415.
 28. Greenwood J, Mason JC. Statins and the vascular endothelial inflammatory response. *Trends Immunol* 2007;28:88–98.